The important role of density in the elastic characterization of reservoirs and it´s computation requirements

Fernando Barbosa da Silva, Andrea Carvalho Damasceno, Matheus Cáfaro Arouca Sobreira, André Eduardo Calazans Matos de Souza, Frederico Alexandre F Oliveira (PETROBRAS/E&P-EXP)

Abstract

This paper addresses two different targets: 1- The importance of the density as a physical property which is very useful in the search and characterization of oil and gas reservoirs and 2- The necessary conditions required in order to obtain a useful and reliable density volume from seismic data elastic inversion.

Introduction

We have observed that it is very common that an oil or gas bearing reservoir doesn´t show a significant compressional velocity (V_p) drop compared to the surrounding rock as would normally be expected. On the order hand, it is possible to verify in many cases that density is decreasing in a significant way, working as a reservoir or hydrocarbon indicator, showing the sensibility of this property to lithology and fluid change.

The general procedure is to avoid working or even trying to obtain the density from seismic data. The reason that explains this behavior comes from the way this parameter is computed. From Zoeppritz derived equations, density appears as a second order term in the computation of the reflection coefficient when expressed in terms of the angle of reflection and the elastic properties of the top and bottom layers.

Nonetheless, a recent work from Behura et al (2010) reported a successful case of density extraction and application.

The target of this work is to stimulate a technical and scientific discussion in order to challenge the people that work not only performing the daily basis seismic inversion as well as the people from basic research, software development, seismic processing and acquisition as long as the interpreters, to look for new work patterns and procedures having in mind this objective.

Examples

The density is normally obtained using solutions for the Zoeppritz equations such as the Aki & Richards approximation (Shuey, 1985) for the reflection coefficient which is given by:

$$R(\theta) \approx R(0) + G\sin^2\theta + F\left(\tan^2\theta - \sin^2\theta\right)$$

where :

$$R(0) = \frac{1}{2}\left(\frac{\Delta V_p}{\bar{V}_p} + \frac{\Delta\rho}{\bar{\rho}}\right) \quad ;$$

$$G = \frac{1}{2}\frac{\Delta V_p}{\bar{V}_p} - 2\frac{\bar{V}_s^2}{\bar{V}_p^2}\left(\frac{\Delta\rho}{\bar{\rho}} - 2\frac{\Delta V_s}{\bar{V}_s}\right) \quad \text{and} \quad F = \frac{1}{2}\frac{\Delta V_p}{\bar{V}_p}$$

R : Reflection coeficient Δ : Diference

θ : incident angle; $\bar{}$: Average

V_p : compressional wave velocity ; V_s : shear wave velocity;

ρ : density

So, $\frac{\Delta\rho}{\bar{\rho}} = R(0) - F$

As it is possible to observe, an accurate estimation of both $R(0)$ and F parameters must be done to obtain density values. The parameter F is great enough to influence R(t) only when the angle is big, as can be observed at Figure 1 where the values of $tg^2(\theta)$-$sin^2(\theta)$ detaches from zero at 20°. The value of this weight for instance is 0.5 for a 45° angle. Then we can extract the first requirement for density estimation: The input data must have a fair amount of coverage over the 30° limit.

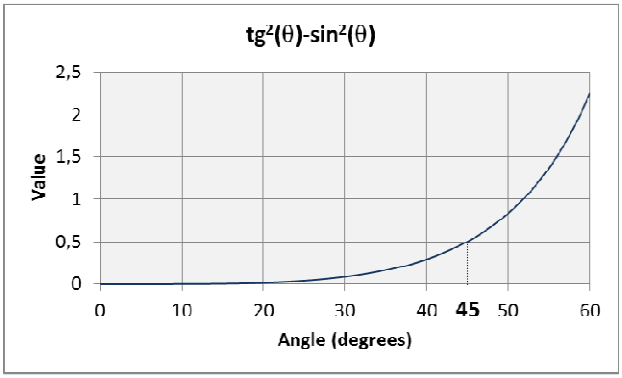

Figure 1: The value of the weight for F versus incident angle.

Another requirement is the significance of the density change with respect to other parameters such as V_p and σ (Poisson ratio) as pointed all by Behura et al (2010). Figures 2 and 3 are good examples of this needed behavior. On both cases it is easy to detect the role of the density as a reservoir indicator specially when the compressional velocity is greater than the background, as in Figure 2, or the Poisson ratio behavior is ambiguous like the one showed in Figure 3.

Although we did not made a compilation of the occurrences in the Brazilian and World context the reader is invited to make his own search and browse around any basin in order to find significant cases that corroborate the point we are rising here.

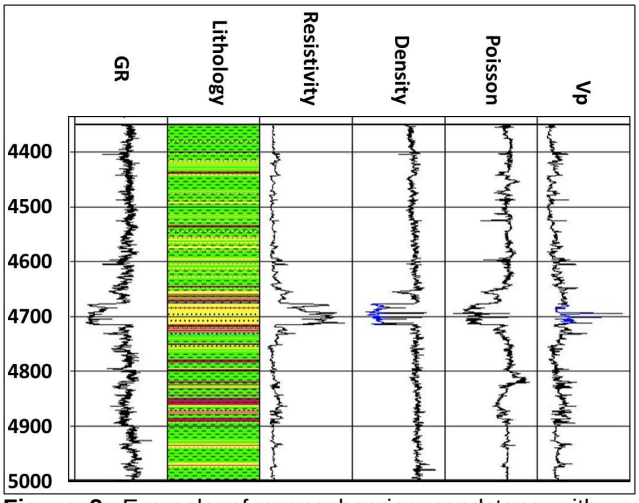

Figure 2: Example of a gas bearing sandstone with decrease in density and Poisson ratio plus V_p increasing at the reservoir layer. Vertical scale is depth, meters.

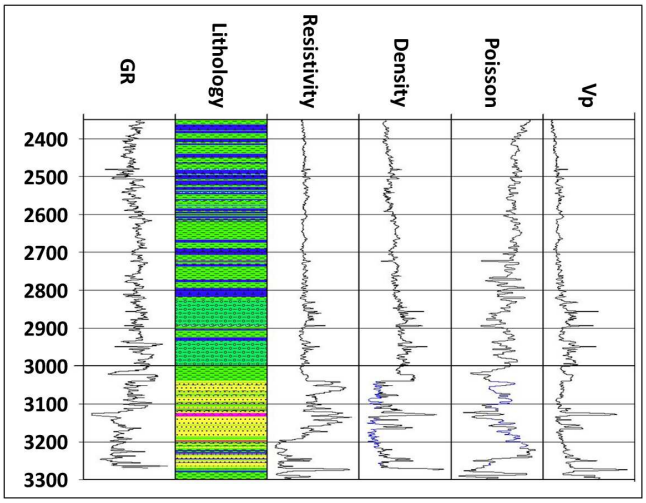

Figure 3: Example of oil bearing sandstone with decrease in density, ambiguous Poisson ratio behavior and subtle V_p decreasing. Vertical scale is depth, meters.

Methodology

In order to demonstrate the main requirements that rule the density extraction we will use synthetic data which are modeled based on real wells.

The first important point that must be investigated is the number of partial stacks used and the signal to noise ratio. In order to check together the role of number of stacks used and maximum angle, individual traces were computed and partial stacks done producing the 3 different inversion cases shown in Table 1 where both the angle spread and number of stacks varies. Case 1 has 3 stacks and goes up to 31°. Case 2 has a maximum angle of 43° and 3 stacks while case 3 has four stacks and angles between 1° and 41°.

Results

The inversion result for these three cases is depicted in Figure 4 where the real density response is compared to the obtained inverted response for the three different cases. It is clear that the output quality increases with both the number of stacks and maximum angle. The better result comes at inversion 3 using a 4 stacked traces input and a maximum angle of 41 degrees. Using the same angle range but staying with only 3 stacks we notice a quality decrease in inversion 2. Just limiting the number of stacks to 3, the delivering capacity is reduced again as can be seen on the inversion 1 result. The reason for the best response is partially due to the ability of the inversion algorithms to fit the output to a greater number of points, which is quite intuitive and easy to understand. The width of the angle range also affects the results. This can be observed in Figure 5 where the stacked traced is compared to the nominal angle trace. The figure shows that the larger the spread, greater is the difference between the two traces. This difference will affect the inversion solution since the input data, which is an average, is already different of the real solution for the assumed angle in the computation.

	ANGLE INTERVAL (°)	AVERAGE ANGLE (°)
Inversion 1	1-11	6
	11-21	16
	21-31	26
Inversion 2	1-15	8
	15-29	22
	29-43	36
Inversion 3	1-11	6
	11-21	16
	21-31	26
	31-41	36

Table 1: Angle range and average for the inversion experiment.

Another aspect that must be considered is the signal to noise ratio. A better result is normally expected for a data with low noise content. This is illustrated using synthetic data and Fatti (1994) solution to Zoeppritz equations where $r(\bar{\theta})$ is the reflection coefficient:

$$r(\bar{\theta}) = A(1+tg^2\bar{\theta})+D\sin^2\bar{\theta} - E\sin^2\bar{\theta}\ tg^2\bar{\theta}$$

Where:

$$A = \frac{1}{2}\left(\frac{\Delta v_p}{v_p} + \frac{\Delta\rho}{\bar{\rho}}\right)$$

$$D = k\left[\frac{\Delta v_s}{v_s} + \left(\frac{1+k}{2k}\right)\frac{\Delta\rho}{\bar{\rho}}\right]$$

$$k = 4\frac{\bar{v}_s^{\,2}}{\bar{v}_p^{\,2}} \quad and \quad E = \frac{1}{2}\frac{\Delta\rho}{\bar{\rho}} \qquad \bar{\ }: \text{average}$$

As anyone can verify the density is directly related to the ***E*** factor on Fatti´s equation. Data was generated in a $0^o \rightarrow 45^o$ range and 1^o step between each trace. Noise

was added as 2%, 5% and 10% amplitude ratios before stack and for each angle trace, as shown in Figure 6. The inversion was performed and Fatti coefficients estimated. The estimations of parameters ***D*** and ***E*** are shown in Figure 7 for 10% and the noiseless cases. Although we perform the same for 2% and 5% of noise it is easier to compare only the two extremes in order to draw the needed conclusions. As was predicted from theory, ***E*** estimation is more affected by noise. This can be better observed when we cross plot the ***D*** and ***E*** values between the 10% noise and noiseless data, shown respectively in Figure 8 and Figure 9. The dispersion is noticeable stronger for ***E*** compared to ***D***, aiding the comprehension of the previous statement.

The last point that we need to address is the way which available commercial inversion software deals with the density question. Considering that they normally assume that:

1. The previously discussed requirements needed in order to achieve fair density estimation has not been satisfied;
2. The density will follow the Gardner (1974) law;
3. The density will not be responsible for both the elastic behavior of the rocks and the seismic response of the data.

Almost often there is a default constraint that imposes the Gardner law over the output result, impeding the work of the system to deliver a density anomaly even when present in the low frequency model. With this knowledge in mind anyone who works with inversion need to find out how his specific tool acts on this explicit topic and find a way to override it providing the proper parameterization. Another consequence is the need or room to new or better tuned software packages that would deal with this requirement in a more adequate way.

Conclusions

As a general conclusion we can state that density is a physical property that can be obtained from seismic data since five requirements are satisfied, to know:

1. The density has a strong contrast with the surrounding rocks.
2. The seismic data has good quality with high signal to noise content.
3. There is a wide angle coverage spreading over the 30° limit.
4. The stack partial data had been properly built in order to ensure the existence of at least 4 angle ranges.
5. Correct inversion parameterization with special attention to internal or hidden constraints such as Gardner law imposition which would limit the decoupling between velocity and density.

It is also important to say again that there is room for the development of new inversion algorithms and programs that will take better care of these particular requirements.

Acknowledgments

We would like to acknowledge our Petrobras managers Raul Damasceno, Paulo Siston and Mario Carminatti for the allowance to spend our time in this work, for the permission to access the data and to publish and present this paper.

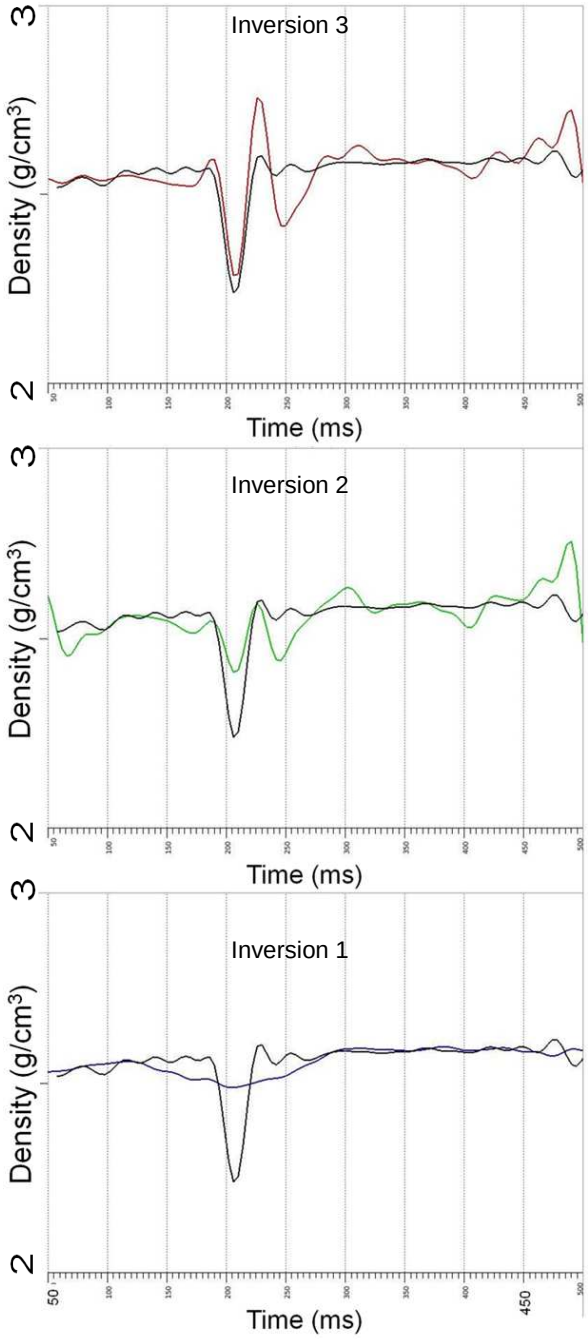

Figure 4: Results for the density inversion for the 3 different inputs. Black is the original filtered density and dark blue, green and red lines are the obtained results from inversion for each case.

References

Behura, J.; Kabir, N.; Crider, R., Jilek P., and Lake E. – Density extraction from P-wave AVO inversion: Tuscaloosa Trend example. The Leading Edge, July 2010, v. 29, p. 772-777.

Fatti, J. L., Smith, G. C., Vail, P. J., Strauss, P. J., and Levitt P. R., 1994, Detection of gas in sandstone reservoirs using AVO analysis: A 3-D seismic case history using the Geostack technique: Geophysics, 59, 1362-1376.

Gardner L.W. & Gregory A.R., 1974, Formation velocity and density - the diagnostic basics for stratigraphic traps. Geophysics 39: 770–780, ()

Shuey, R.T. –A Simplification of the Zoeppritz Equations. GEOPHYSICS, v. 50, no. 4 (April 1985), p. 609–614.

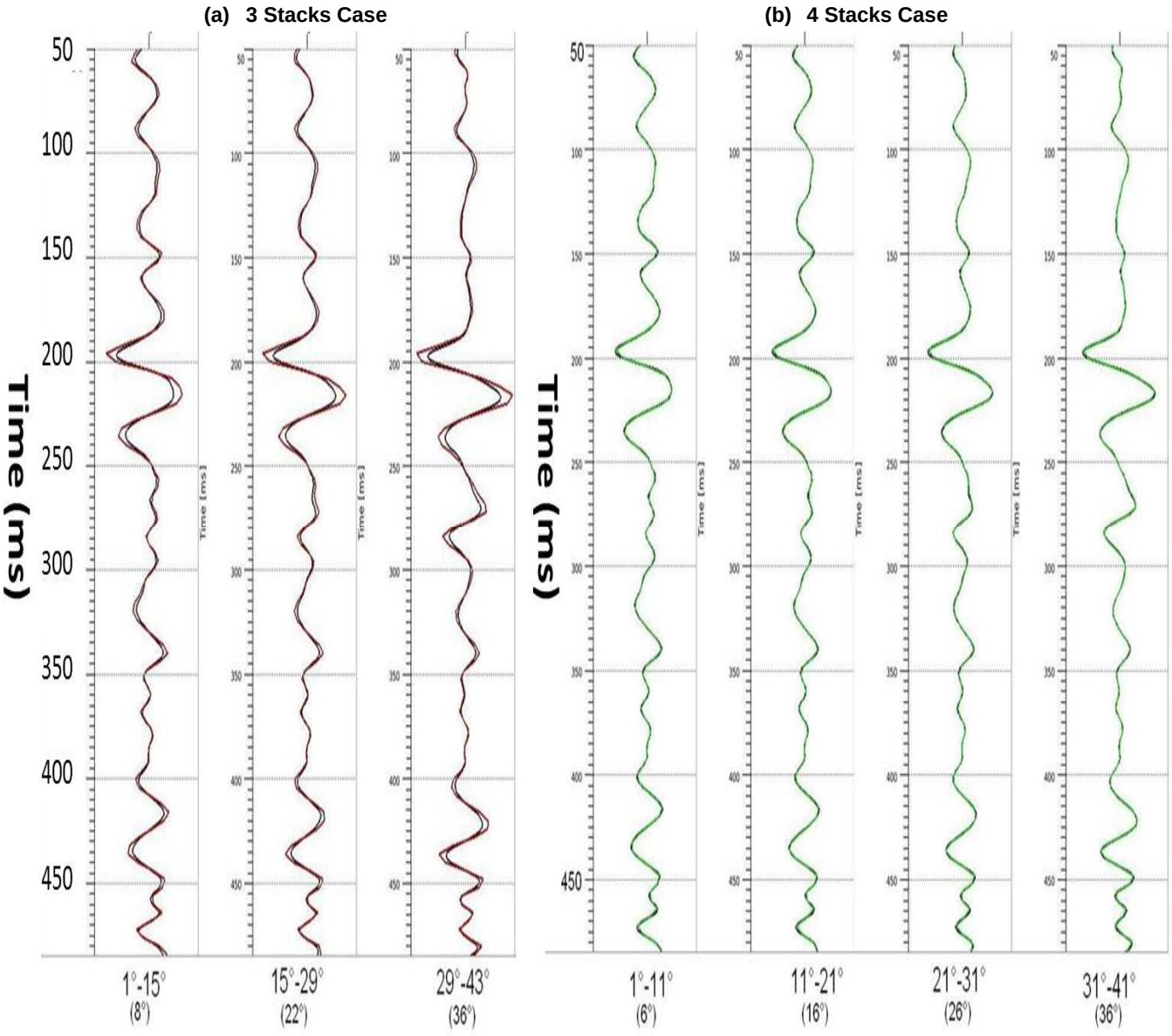

Figure 5: Comparison between the stacked trace and the computed synthetic trace assumed for the inversion computation. Computed traces are depicted in black and stacked in red for the 3 partial stacks case (a) and green for the 4 partial stacks case (b). Note that for the second case the computed trace is imperceptible because it is behind the stacked.

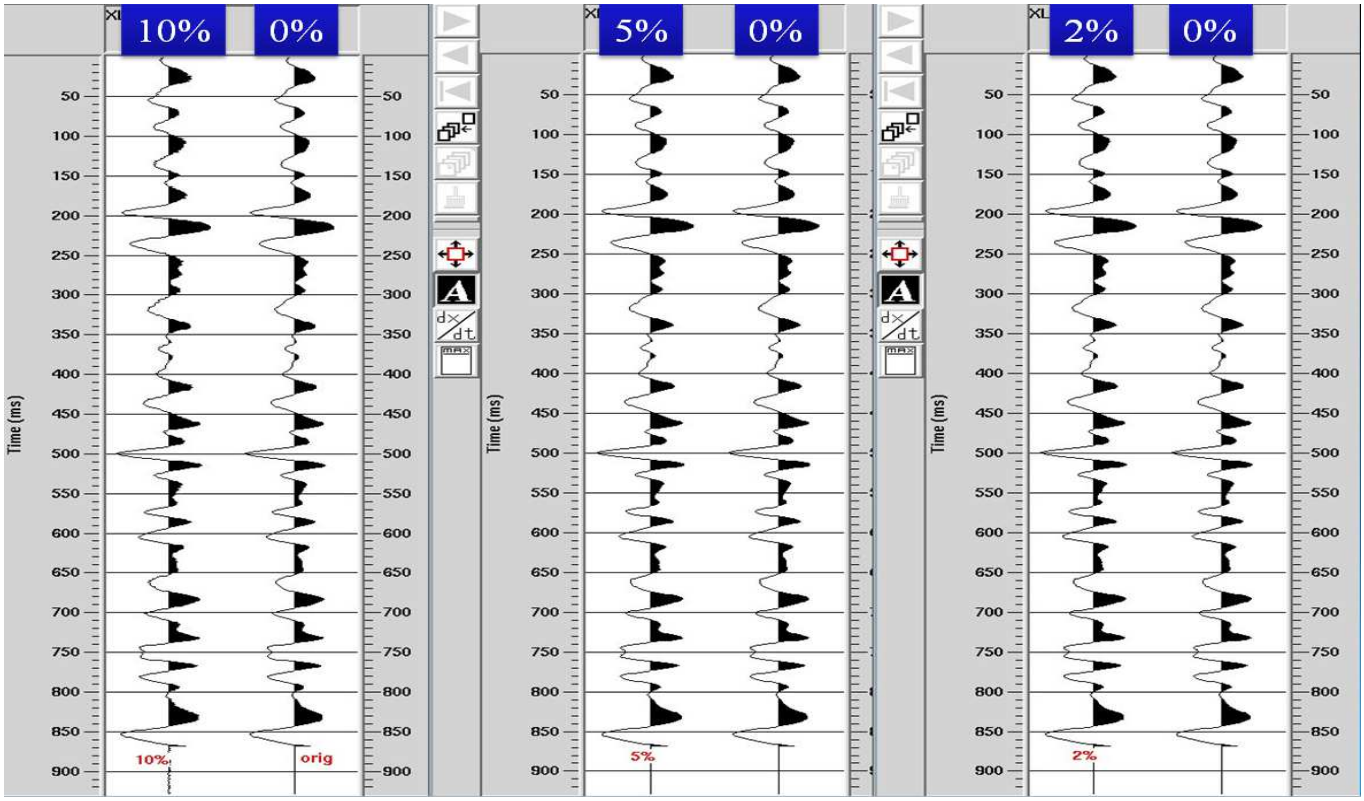

Figure 6: Computed trace at 15º angle compared to added noise version at 10%, 5% and 2%.

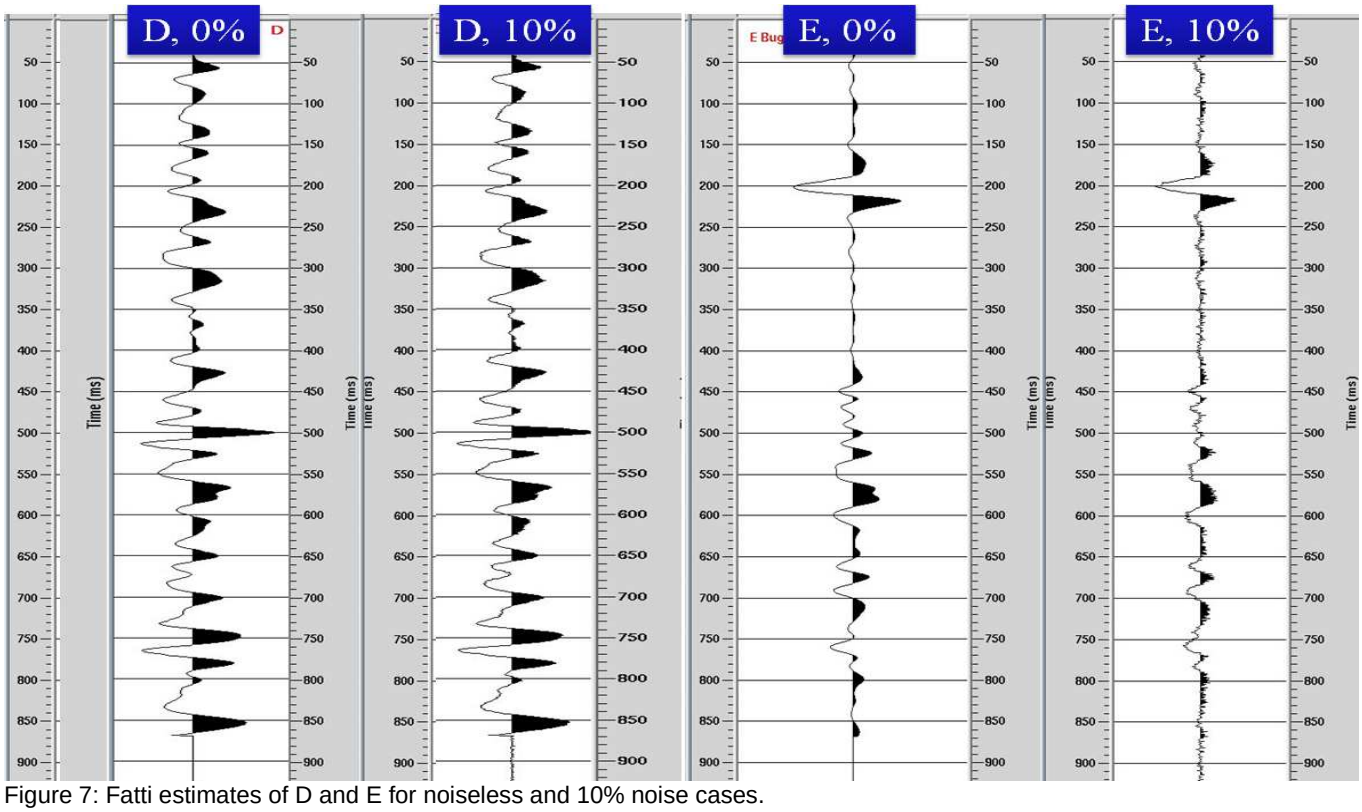

Figure 7: Fatti estimates of D and E for noiseless and 10% noise cases.

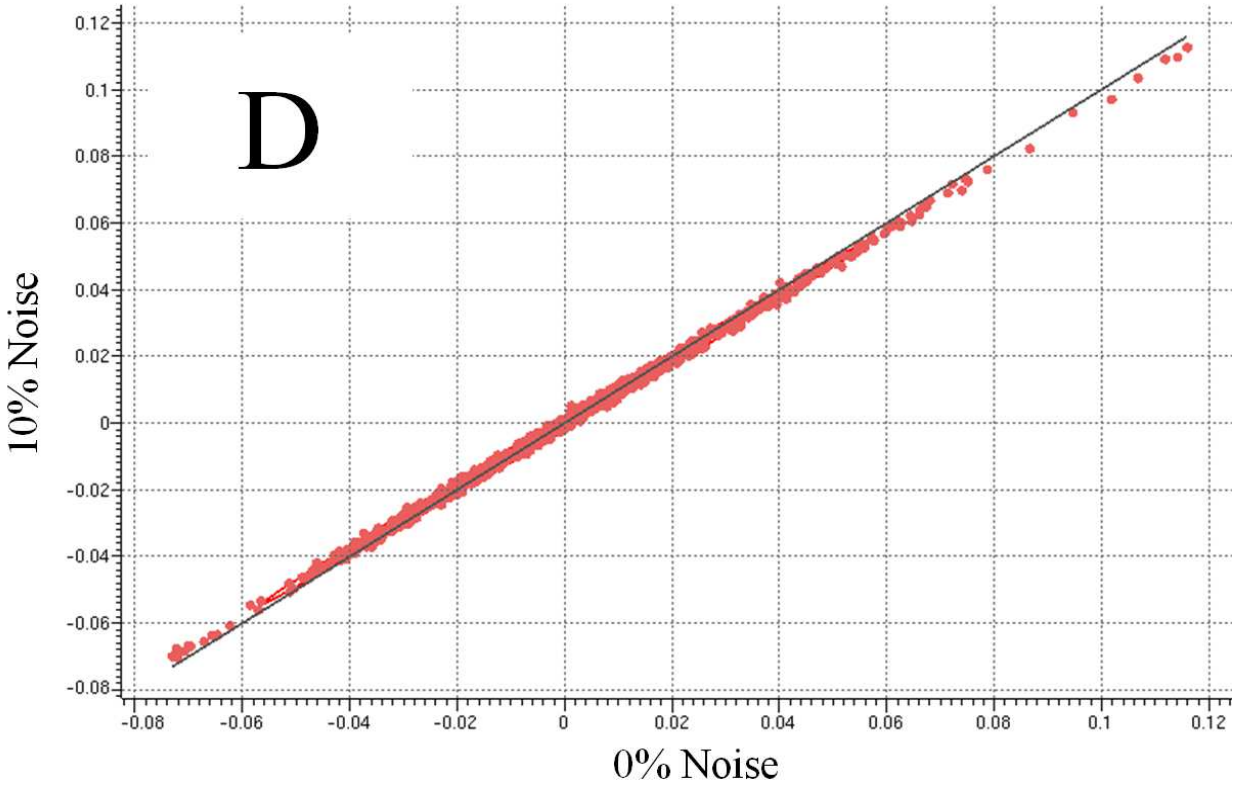

Figure 8: Cross plot of D factor between 10% noise case and noiseless data.

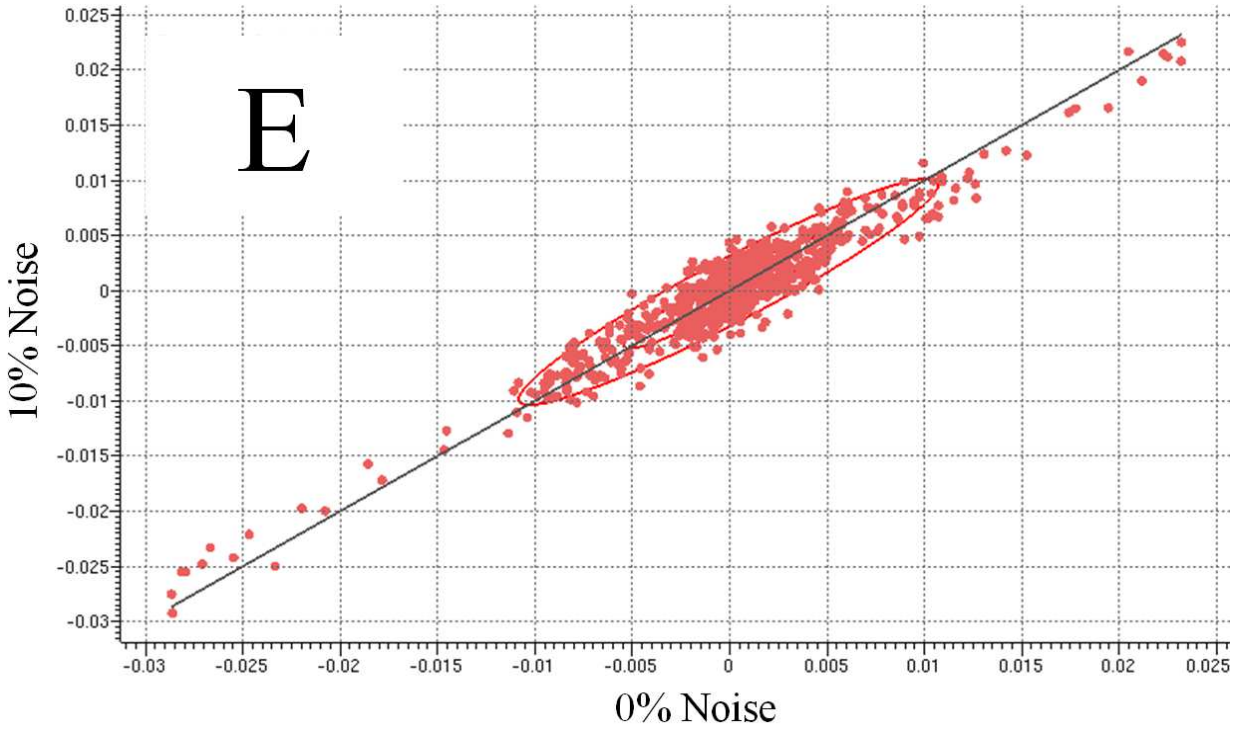

Figure 9: Cross plot of E factor between 10% noise case and noiseless data.